Production of n and $\bar{n}$ in $\pi^- p$ and π^-Ne collisions at 200 GeV/c*

L. R. Fortney, A. T. Goshaw, J. W. Lamsa, J. S. Loos, W. J. Robertson, and W. D. Walker
Physics Department, Duke University, Durham, North Carolina 27706
(Received 29 March 1976)

The processes $\pi^- p \rightarrow$(neutral hadron) + X and π^-Ne$\rightarrow$(neutral hadron) + X at 200 GeV/c have been studied and compared by examining the secondary collisions of neutral hadrons in a bubble chamber. The results are satisfactorily explained in terms of n and $\bar{n}$ production. The observed $\bar{n}$ production rates are 0.10 ± 0.04 per inelastic $\pi^- p$ collision and 0.07 ± 0.03 per inelastic π^-Ne collision. No evidence for new long-lived neutral hadrons is found.

I. INTRODUCTION

During the past few years, a great deal of experimental and phenomenological work has been devoted to the properties of neutral-particle production in high-energy collisions. The experimental work has been concentrated on those neutral particles ($\gamma, \pi^0, K^0, \Lambda^0$) which produce readily identifiable signatures. Neutron production has been reported only in a few instances in proton-induced reactions,[1,2] and not at all in pion-induced reactions. There exists no experimental information on antineutron production at high energies. The intriguing possibility of the production at high energies of a long-lived ($\gtrsim 10^{-8}$ sec) neutral hadron (with or without "charm" or "color" quantum numbers) also remains unexplored.

In the present experiment we have investigated the production of n and $\bar{n}$ particles, and have searched for the presence of any other long-lived particles by studying the following reactions at 200 GeV/c:

$$\pi^- p \rightarrow (\text{neutral hadron}) + X,$$

$$\pi^-\text{Ne} \rightarrow (\text{neutral hadron}) + X,$$

where the neutral hadrons are observed by their subsequent hadronic interactions. No evidence for the existence of a new long-lived neutral hadron is found. The data are interpreted satisfactorily in terms of the inclusive reactions

$$\pi^- p \rightarrow n X$$
$$\rightarrow \bar{n} X,$$
$$\pi^-\text{Ne} \rightarrow n X$$
$$\rightarrow \bar{n} X.$$

In addition to the inherent interest in n and $\bar{n}$ production, the present study provides interesting comparisons between production from a nucleon target and production from a nuclear target at high energy.

The results are based on a 50 000 picture exposure of the Fermi National Accelerator Laboratory 30-in. bubble chamber filled with a mixture of H_2 and Ne consisting of 31 molar percent Ne. The probability of detecting a neutral hadron in this mixture is approximately three times as large as for a pure H_2 fill.

II. FILM ANALYSIS PROCEDURES

A. Film sample and interaction region

In order to obtain a clean sample of photographs, a photograph was rejected whenever any nonbeam track entered the interaction region or whenever there were two or more beam interactions within the interaction region. These cuts were quite effective in minimizing possible confusion arising from neutral hadrons produced anywhere upstream of the interaction region or from multiple beam interactions in a frame (see Sec. II C below). Approximately 30 000 of the 50 000 photographs survived these cuts and were then scanned at a magnification of 1.4 times life size.

The interaction region for the π^- beam was chosen to be 25 cm long. This choice allowed an average length of about 50 cm for determination of the multiplicity and charge information from the crowded forward tracks.

B. Separation of events into $\pi^- p$ and π^-Ne collisions

A total of 5047 π^- beam interactions were found. For each event the scanner recorded N_h, the number of heavily ionizing tracks (mainly protons having $p_{\text{lab}} < 1.0$ GeV/c), and n_s, the number of "shower" tracks (minimum ionizing tracks plus identified pions). The shower-track curvatures were then used to count the number of positively and negatively charged shower tracks, n_+ and n_-. A small fraction of the shower tracks were too energetic ($p_{\text{lab}} \gtrsim 75$ GeV/c) to assign charge, but this was not a serious problem.[3]

A separation into $\pi^- p$ (hydrogenic) and π^-Ne (neonic) events was then made. Hydrogenic events

were required to have even multiplicity, net charge consistent with zero, and either 0 proton or 1 proton having a track length and production angle kinematically consistent with a $\pi^- p$ collision. Of the 5047 events, only 187 (2%) were unclassifiable because of a close secondary interaction or some other problem. Of the remaining 4860 events, 1747 were classified as hydrogenic and 3113 as neonic. On the basis of the known liquid composition and the known total cross sections, we expect that 1361 of the hydrogenic events are true $\pi^- p$ interactions. The excess hydrogenic events are predominantly π^- collisions with a peripheral nucleon in the Ne nucleus, where the remainder of the nucleus acts as a "spectator." These peripheral collisions appear to have the same properties as $\pi^- p$ collisions, and we assume that their inclusion causes no significant bias. For all distributions presented in this paper, an overall normalization correction has been applied to compensate for this misclassification between hydrogenic and neonic events.

A test of the separation procedure is shown in Fig. 1, where we compare the multiplicity distribution of the hydrogenic events with the published $\pi^- p$ result at the same energy.[4] Since no significant differences are seen at any multiplicity, we conclude that the separation procedure is quite reliable.

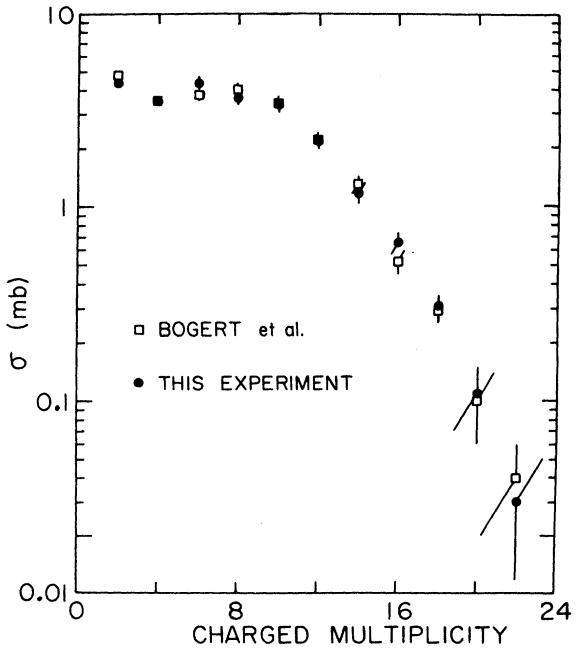

FIG. 1. Charged multiplicity cross sections for the selected hydrogenic events (circles), compared to the published results of Ref. 4 at $\pi^- p$ at 200 GeV/c (squares). An overall normalization correction has been made to the data from the present experiment.

C. Scan procedure for neutral hadron interactions

The 4860 photographs corresponding to observed π^- interactions were then rescanned for the presence of "hadron stars" (produced by the interaction of a neutral hadron) anywhere within the chamber. A second scan for hadron stars, done over 30% of the sample, established a scanning efficiency of 93% for finding the stars. One-prong stars and two-prong stars with zero net charge (V's) were excluded. The average potential length for observing a star was 45 cm. For each star found, the scanner recorded n_s and N_h at the star vertex, and measured the projected production angle of the neutral particle in two views.

The scan results, together with various cuts and corrections, are summarized in Table I. A total of 491 star candidates were recorded. Of these, 432 survived cuts on the chamber volume and were subsequently examined at the scan table by a physicist in an effort to ascertain the production origin of each star candidate. The only significant ambiguity of hadron-star origin was caused by secondary interactions of outgoing charged particles. A total of 312 stars were classified as having a clean or probable association with the primary vertex, 40 stars were rejected as unassociated with the primary vertex, and 80 stars were classified as having an ambiguous origin. Of the latter category, it is estimated that 34 are associated with a primary interaction and that 46 are associated with a secondary interaction on an outgoing track.

A special scan to search for random hadron stars arising from undetected interactions in or upstream of the bubble-chamber window was also

TABLE I. Summary of scan results for neutral hadron stars.

Number of observed hadron stars	491
Number surviving chamber volume cuts	432
Classification of surviving stars:	
Clean or probable association	312
Ambiguous association	80
Rejected as unassociated	40
Corrections:	
For loss due to ambiguous association	34
For loss due to scan efficiency	24
Corrected number of hadron stars in the data sample (312+34+24)	370 [a]
Number from $\pi^- p$ interactions	100 [a]
Number from π^-Ne interactions	270 [a]

[a] These are the corrected number of observed hadron stars caused by n, $\bar{n}$, K^0, $\bar{K}^0$, or other neutral hadrons.

performed on a sample of 5000 photographs having no beam interaction in the interaction region. (These 5000 photographs formed a subset of the 30 000 clean photographs mentioned in Sec. II A.) Two such random hadron stars were found. We conclude that this is a negligible background for the present experiment which uses a π^- beam.

III. RESULTS AND DISCUSSION

A. Kinematical considerations of the variable η

The laboratory production angle, θ, of each hadron star has been reconstructed from its projection in two views. The analysis of the data has then been done by using the variable η, defined as

$$\eta \equiv -\ln(\tan\tfrac{1}{2}\theta).$$

A few kinematical aspects of the variable η should be noted. For zero-mass particles, η is identical to the laboratory rapidity, y_{lab}. The approximation, $\eta \simeq y_{lab}$, is quite good for π mesons. However, for higher-mass particles η is shifted to higher values by an amount which depends upon the transverse momentum of the produced particle. This is illustrated in Fig. 2, where we display curves of η versus y_{lab} for neutrons produced with various values of p_T. Although a given value of η is seen to span a range of values of y_{lab}, the average rapidity, $\bar{y}_{lab}$, can be computed if the transverse momentum distribution is known for the produced particle. The dashed curve of Fig. 2 shows $\bar{y}_{lab}$ versus η for neutrons produced in the present experiment. This curve has been calculated by assuming a transverse-momentum distribution proportional to $\exp(-4p_T^2)$, consistent with published results.[5,6] The same calculation also provides the correspondence between η and $\bar{p}_{lab}$ for the produced neutrons, as indicated by the upper horizontal scale in Fig. 2. Note that on the average the zero of $y_{c.m.}$ corresponds to $\eta = 4.0$ and to $\bar{p}_{lab} = 10.0$ GeV/c for neutrons (or antineutrons) produced in the present experiment.

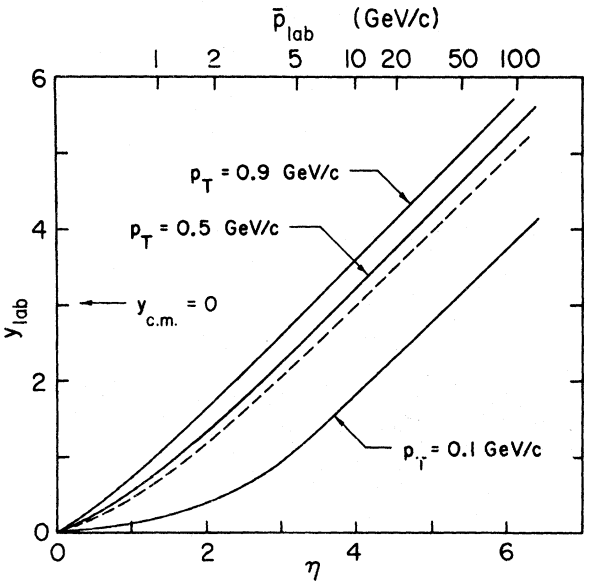

FIG. 2. Kinematical relations between the variable η and the laboratory rapidity, y_{lab}, for neutrons (or antineutrons) produced with the indicated values of transverse momentum. The dashed curve shows the relation between η and the average rapidity, $\bar{y}_{lab}$, for this experiment (see text). The upper scale also shows the correlation between η and the average laboratory momentum of the neutron.

B. η distributions

The observed η distributions for both the π^-p and π^-Ne events are shown in Fig. 3. The solid curves are estimates of the expected contributions from

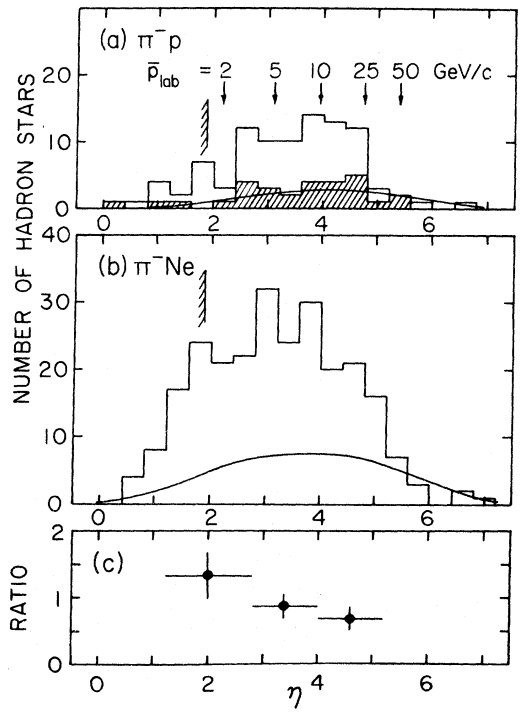

FIG. 3. Observed η distributions for hadron stars from (a) π^-p events and from (b) π^-Ne events. The average values of the laboratory momentum versus η, shown by the arrows, are computed by assuming the neutral particle to be a neutron. Detection efficiencies are not reliably known to the left of the vertical shaded bar. The expected K^0 and $\bar{K}^0$ contributions are shown by the solid curves (see text). The shaded events are those for which a proton track is identified by track density. (c) Ratio of the number of hadron stars per π^-Ne interaction to that per π^-p interaction (K^0 and $\bar{K}^0$ stars removed).

K^0- or $\bar{K}^0$-induced stars, made on the basis of a Monte Carlo calculation which simulated known K^0 and $\bar{K}^0$ production properties[7-10] and the effects of the finite chamber volume. These calculations indicate that 24% and 30% of the hadron stars from $\pi^- p$ and π^-Ne collisions, respectively, are caused by K^0 or $\bar{K}^0$ interactions. The contributions expected from Λ^0- or Σ^0-induced stars have been ignored.[11] The major portion of the hadron stars, therefore, are produced by neutral particles other than K^0, $\bar{K}^0$, or Λ^0.

There are several interesting features to be noticed in Fig. 3 assuming for the moment that the observed hadron stars are produced by neutrons and antineutrons. Production in the backward center-of-mass hemisphere ($\eta < 4$) is clearly seen to be much larger than in the forward hemisphere. However, ~25% and ~20% of the observed stars are produced in the forward hemisphere ($\eta > 4$) for $\pi^- p$ and π^-Ne interactions, respectively. It seems unlikely that such large percentages can result solely from neutrons produced by target fragmentation. Both the $\pi^- p$ and π^-Ne events in the forward hemisphere occur within about 1 rapidity unit of the zero of $y_{\text{c.m.}}$, and both data are consistent with no long-lived neutral particles being produced in the beam fragmentation region (when K^0 and $\bar{K}^0$ are removed). These features can be understood if there are two distinct contributions: (1) an n component from target fragmentation, and (2) smaller components of n and $\bar{n}$ arising from $N\bar{N}$ pair production in the central region of rapidity ($-1 \lesssim y_{\text{c.m.}} \lesssim 1$). A quantitative interpretation of the data in terms of these contributions is made in Sec. III D below.

There are two pieces of direct evidence to suggest that $N\bar{N}$ production is important. First, the shaded events in Fig. 3(a) are $\pi^- p$ events which have a visually identified proton at the primary interaction (laboratory momentum less than 1.0 GeV/c). Therefore, the hadron star in these events cannot be caused by a neutron originating from a charge-exchange reaction. (Only 25% of the shaded events are expected to be K^0 or $\bar{K}^0$ stars.) Second, we find three examples from the $\pi^- p$ events and nine from the π^-Ne events where two hadron stars are observed in the same event. (A total of only four of these cases is expected to arise from events having a K^0 or $\bar{K}^0$ star.)

A direct comparison between the production from π^-Ne versus that from $\pi^- p$ is made in Fig. 3(c), where we have plotted the ratio of neutral-hadron production per π^-Ne collision to that per $\pi^- p$ collision (K^0 and $\bar{K}^0$ removed). In going from the central region to the target fragmentation region, the production from the nuclear target gradually becomes more important than that from the nucleon target. This trend can be simply understood by noting that on the average more than one nucleon participates in a nuclear collision.

C. Shower-track multiplicities at the star vertex and at the primary vertex

For each bin of η, we have measured the average shower multiplicity at the star vertex, $\bar{n}_s$. Following the method outlined in Sec. III A above, we also computed $\bar{p}_{\text{lab}}$, the average laboratory momentum of the neutral hadron (assumed to be a neutron or antineutron). The dependence of $\bar{n}_s$ on $\bar{p}_{\text{lab}}$ (see Fig. 4) is found to be consistent with the relation

$$\bar{n}_s = 0.17 + 1.93 \ln \bar{p}_{\text{lab}}$$

over the interval $2 \lesssim \bar{p}_{\text{lab}} \lesssim 25$ GeV/c. The logarithmic growth of multiplicity with bombarding energy agrees well with what is expected from previous work. For comparison, the average charged multiplicity for pp interactions above 6 GeV/c is given by[12]

$$(\bar{n}_{\text{ch}})_{pp} \simeq -0.75 + 1.5 \ln p_{\text{lab}} .$$

We note that for a given p_{lab}, the values of $\bar{n}_s$ are expected to be somewhat larger than the values of $(\bar{n}_{\text{ch}})_{pp}$ because the neutral hadron stars occur primarily on Ne nuclei.[13] The observed behavior of $\bar{n}_s$ serves as a valuable check of our overall procedures.

It is of interest to see whether the shower multiplicity at the primary vertex depends upon whether or not a hadron star is produced. In Fig. 5, we display $\bar{n}_s$ at the primary vertex for various bins of η, both for π^-Ne interactions (solid squares) and for $\pi^- p$ (open circles). The overall average multiplicity of shower tracks produced at the primary interaction for events having an associated hadron star is 9.1 ± 0.3 for $\pi^- p$ events and 12.7

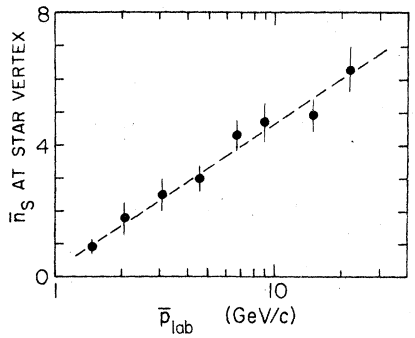

FIG. 4. Average shower multiplicity at the star vertex versus the average value of p_{lab}. The values of $\bar{p}_{\text{lab}}$ are computed by assuming the neutral hadron to have the mass of a neutron (see text). The dashed line is a fit given by $\bar{n}_s = 0.17 + 1.93 \ln \bar{p}_{\text{lab}}$.

± 0.4 for π^-Ne events. These numbers are independent of η and are significantly higher than the corresponding values, 6.9 ± 0.1 and 9.6 ± 0.1, for all events. This result would seem to imply that collisions which produce relatively energetic n or $\bar{n}$ particles are more violent than the average collision, and therefore usually lead to a higher than average multiplicity.

D. Interpretation of results in terms of n and $\bar{n}$ production

A quantitative interpretation of the data has been made by using a Monte Carlo simulation to evaluate the n and $\bar{n}$ detection probabilities and to unfold the $y_{\text{c.m.}}$ spectrum from the η spectrum. In the calculation, the particles were generated by assuming a transverse-momentum distribution proportional to $\exp(-4p_T^2)$, as discussed in Sec. III A. The average probability of a subsequent detectable star within the scanning volume was evaluated from the known geometry and from the known absorption cross sections.[14-16] The resulting average n and $\bar{n}$ detection probabilities for the present experiment are shown in Fig. 6. At low energies, antineutrons are more readily detected than neutrons because of the annihilation processes. In the region $\eta \gtrsim 2$ (corresponding to $\bar{p}_{\text{lab}} \gtrsim 2$ GeV/c), the calculated detection probabilities are quite reliable.

Unfortunately, there is no easy way to distinguish individually n stars from $\bar{n}$ stars because they usually look similar in the bubble chamber. However, a range of estimates for separate n and $\bar{n}$ production has been made by considering two sets of assumptions (case 1 and case 2). For both cases, we assume that all the hadron stars are caused by n or $\bar{n}$ (when K^0 and $\bar{K}^0$ are removed) and that the $\bar{n}$ component arises from a nonfragmentation process that is symmetric about the zero of $y_{\text{c.m.}}$.

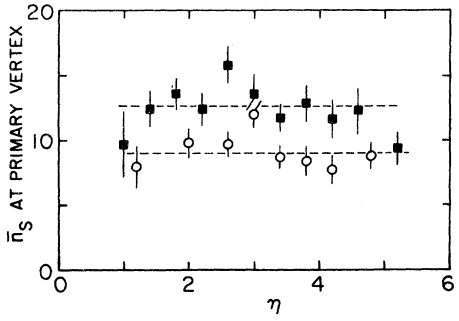

FIG. 5. Average shower multiplicity at the primary vertex versus η for events having an associated hadron star. The π^-Ne events (solid squares) and the π^-p events (open circles) have average shower multiplicities of 12.7 ± 0.4 and 9.1 ± 0.3, respectively, as indicated by the dashed lines.

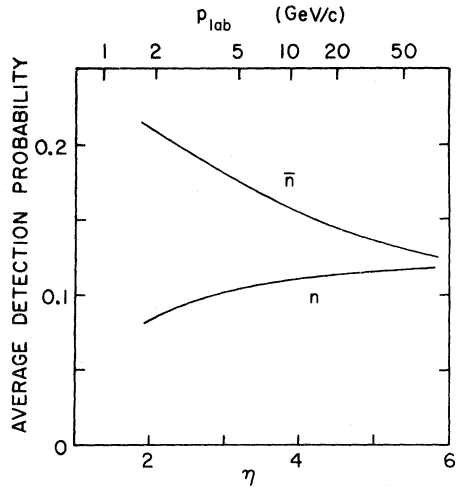

FIG. 6. Average detection probabilities for n and $\bar{n}$ versus the variable η for the present experiment.

For case 1, we further assume that the n contribution from target fragmentation is negligible for $y_{\text{c.m.}} > 0$, whereas for case 2 we assume that 5% of all target fragmentation occurs in the region $y_{\text{c.m.}} > 0$, consistent with data at low energy.[17]

In Fig. 7, we show the n-production cross sections derived from the η distributions using the calculated detection probabilities and the assumptions outlined above. The solid circles refer to case 1 and the broken circles refer to case 2. The

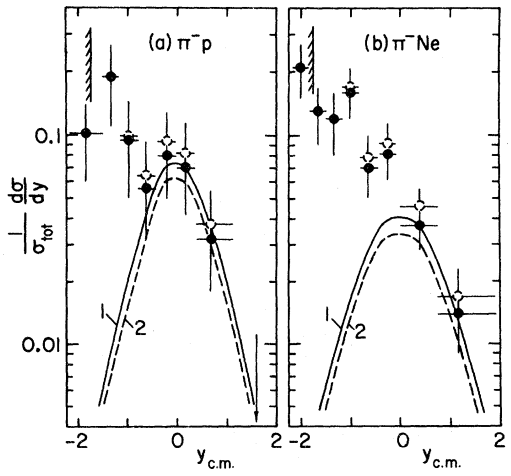

FIG. 7. Estimates for n and $\bar{n}$ production cross sections for (a) π^-p and (b) π^-Ne interactions. The solid circles and broken circles, respectively, represent n production for the assumptions of case 1 and case 2 (discussed in the text). The corresponding $\bar{n}$ production is given by the solid (dashed) hand-drawn curve for case 1 (case 2). The error bars represent statistical uncertainties. Detection efficiencies are not reliably known to the left of the vertical shaded bar.

range of values spanned by the two cases are within the statistical errors of this experiment. The corresponding estimates for $\bar{n}$ arising from $N\bar{N}$ production are shown as smooth curves (solid curve for case 1, dashed curve for case 2). This analysis gives 0.10 ± 0.04 $\bar{n}$ per $\pi^- p$ collision and 0.07 ± 0.03 $\bar{n}$ per π^-Ne collision. These values are slightly larger than, but consistent with, the reported value of 0.05 ± 0.01 $\bar{p}$ per pp collision at the same center-of-mass energy.[5]

The conclusion of this analysis in that the observed neutral hadrons are n and $\bar{n}$ produced by (1) fragmentation of the target, and (2) $N\bar{N}$ production in the central region of rapidity. We note that the production rates (per collision) from a nucleon target and from a nuclear target are nearly equal in the forward hemisphere. Another interesting result is the absence of any substantial long-lived-neutral-particle production in the beam fragmentation region ($1 < y_{\text{c.m.}} < 3$). Assuming equal $\bar{n}$ and $\bar{p}$ production at high energy, the results quoted in the preceding paragraph imply that the production of any new neutral hadron having an interaction cross section comparable to that of a neutron is smaller than about 0.05 particles per event in the region $y_{\text{c.m.}} \gtrsim 0$.

IV. SUMMARY

The main results of the experiment are as follows.

(1) The observed neutral hadron stars can be satisfactorily understood in terms of n and $\bar{n}$ production.

(2) The n and $\bar{n}$ production appears to be the result of both target fragmentation and $N\bar{N}$ production in the central region of rapidity.

(3) The production rates of antineutrons in the central region of rapidity are 0.10 ± 0.04 $\bar{n}$ per $\pi^- p$ collision and 0.07 ± 0.03 $\bar{n}$ per π^-Ne collision, consistent with being equal.

(4) By comparing with $\bar{p}$ production in pp collisions at the same energy, an upper limit has been found of 0.05 particles per collision for the production of any new long-lived ($\gtrsim 10^{-8}$ sec) neutral hadron, provided such hadrons have interaction cross sections comparable to that of a neutron.

(5) The events with associated hadron stars have average shower-track multiplicities roughly 30% higher than the average for all collisions. This result holds for both $\pi^- p$ and π^-Ne.

ACKNOWLEDGMENTS

We thank L. Voyvodic, R. Walker, and the members of the 30-in. bubble-chamber staff for their assistance. We also are grateful for the diligent effort of the scanning staff at Duke, with special thanks to M. Kumar.

---

*Work supported in part by the U. S. Energy Research and Development Agency, and in part by the Duke University Research Council.

[1]F. T. Dao *et al.*, Phys. Rev. D 10, 3588 (1974).

[2]J. Engler *et al.*, Nucl. Phys. B64, 173 (1973).

[3]The problem of undetermined charge of the energetic tracks occurs mainly in the low-multiplicity events where it is common for pions to be produced with p_{lab} in excess of 75 GeV/c. The percentages of all events having 0, 1, or ≥ 2 such energetic tracks were found to be 44%, 43%, and 13%, respectively.

[4]D. Bogert *et al.*, Phys. Rev. Lett. 31, 1271 (1973).

[5]M. Antinucci *et al.*, Lett. Nuovo Cimento 6, 121 (1973).

[6]P. Capiluppi *et al.*, Nucl. Phys. B79, 189 (1974).

[7]For $\pi^- p$ interactions, the Monte Carlo calculation assumed that 0.17 K_S^0 and 0.17 K_L^0 per inelastic collision are produced, consistent with the results of Ref. 8 and Ref. 9. The shape of the rapidity distribution of the produced K^0 particles was assumed to be the same as that for the average of the π^+ and π^- production in $\pi^- p$ interactions at 200 GeV using the unpublished data of the Notre Dame-Canada-Duke collaboration. For π^-Ne interactions, a somewhat higher K^0 production was assumed (0.23 K_S^0 and 0.23 K_L^0 per inelastic collision), where the additional K^0 particles for the nuclear target were taken to occur in the backward hemisphere, consistent with the observed π production from a Ne target reported in Ref. 10.

[8]D. Bogert *et al.*, NAL-Conf-74/55-EXP [submitted to the XVII International Conference on High Energy Physics, London, 1974 (unpublished)].

[9]M. Alston-Garnjost *et al.*, Phys. Rev. Lett. 35, 142 (1975).

[10]W. M. Yeager, Ph.D. thesis, Duke University, 1976 (unpublished).

[11]The number of Λ^0- or Σ^0-induced stars is only about 25% of the number of K^0 or $\bar{K}^0$ stars. (See Ref. 1, for example.) The Λ^0 and Σ^0 stars also contribute mainly to the backward hemisphere ($\eta < 4$).

[12]V. V. Ammisov *et al.*, Phys. Lett. 42B, 519 (1972).

[13]J. R. Elliott *et al.*, Phys. Rev. Lett. 34, 607 (1975).

[14]E. Bracci *et al.*, Report No. CERN/HERA 73-1, 1973 (unpublished).

[15]J. C. Allaby *et al.*, Yad. Fiz. 12, 538 (1970) [Sov. J. Nucl. Phys. 12, 295 (1971)].

[16]R. J. Abrams *et al.*, Phys. Rev. D 4, 3235 (1971).

[17]In $\pi^\pm$Ne interactions at 10.5 GeV/c, Ref. 10 reports that approximately 7% of all protons occur with $y_{\text{c.m.}} > 0$. In $\pi^+ p$ at 15.5 GeV/c, Ref. 18 reports that approximately 3.5% of all protons occur with $y_{\text{c.m.}} > 0$.

[18]M. J. Delay *et al.*, Phys. Rev. D 11, 975 (1975).